Ecological consequences of early Late Pleistocene megadroughts in tropical Africa

Andrew S. Cohen*†, Jeffery R. Stone‡, Kristina R. M. Beuning§, Lisa E. Park¶, Peter N. Reinthal‖, David Dettman*, Christopher A. Scholz**, Thomas C. Johnson††, John W. King‡‡, Michael R. Talbot§§, Erik T. Brown††, and Sarah J. Ivory§

Departments of *Geosciences and ‖Ecology and Evolutionary Biology, University of Arizona, Tucson, AZ 85721; ‡Department of Geosciences, University of Nebraska, Lincoln, NE 68588; §Department of Biology, University of Wisconsin, Eau Claire, WI 54702; ¶Department of Geology, University of Akron, Akron, OH 44325; **Department of Earth Sciences, Syracuse University, Syracuse, NY 13244; ††Large Lakes Observatory and Department of Geological Sciences, University of Minnesota, Duluth, MN 55812; ‡‡Graduate School of Oceanography, University of Rhode Island, Narragansett, RI 02882; and §§Department of Earth Sciences, University of Bergen, N-5007 Bergen, Norway

Edited by David Hodell, University of Florida, Gainesville, FL, and accepted by the Editorial Board August 27, 2007 (received for review April 30, 2007)

Extremely arid conditions in tropical Africa occurred in several discrete episodes between 135 and 90 ka, as demonstrated by lake core and seismic records from multiple basins [Scholz CA, Johnson TC, Cohen AS, King JW, Peck J, Overpeck JT, Talbot MR, Brown ET, Kalindekafe L, Amoako PYO, *et al.* (2007) *Proc Natl Acad Sci USA* 104:16416–16421]. This resulted in extraordinarily low lake levels, even in Africa's deepest lakes. On the basis of well dated paleoecological records from Lake Malawi, which reflect both local and regional conditions, we show that this aridity had severe consequences for terrestrial and aquatic ecosystems. During the most arid phase, there was extremely low pollen production and limited charred-particle deposition, indicating insufficient vegetation to maintain substantial fires, and the Lake Malawi watershed experienced cool, semidesert conditions (<400 mm/yr precipitation). Fossil and sedimentological data show that Lake Malawi itself, currently 706 m deep, was reduced to an ≈125 m deep saline, alkaline, well mixed lake. This episode of aridity was far more extreme than any experienced in the Afrotropics during the Last Glacial Maximum (≈35–15 ka). Aridity diminished after 95 ka, lake levels rose erratically, and salinity/alkalinity declined, reaching near-modern conditions after 60 ka. This record of lake levels and changing limnological conditions provides a framework for interpreting the evolution of the Lake Malawi fish and invertebrate species flocks. Moreover, this record, coupled with other regional records of early Late Pleistocene aridity, places new constraints on models of Afrotropical biogeographic refugia and early modern human population expansion into and out of tropical Africa.

cichlid evolution | Lake Malawi | Out-of-Africa Hypothesis | paleoclimate | paleolimnology

Long, continuous records of Pleistocene paleoecological change in Africa are rare, despite their importance for addressing paleoclimatic, biogeographic, and evolutionary controversies in the tropics (1, 2). For Africa, understanding of Pleistocene environmental history comes from a variety of wetland, lake core, and outcrop records (3–7), which are of geologically short duration and/or low stratigraphic resolution, as well as from analyses of deep-sea cores (8, 9), which integrate information from large areas. To evaluate hypotheses about environmental history at the landscape scale (≈10^4–10^6 km^2), and their potential influence on species' distribution and diversification histories (10), there is a need for records that merge the continuity and duration of deep-sea cores with the relatively rapid sedimentation and high temporal resolution found in lakes.

Here we describe paleoecological results from drill cores recently collected at Lake Malawi, a large (29,500 km^2), deep (706 m) African rift lake located in the southern African tropics (9°–14°S). Today, Lake Malawi lies close to the southern extent of the Intertropical Convergence Zone. The lake's watershed experiences a mesic climate, with highly seasonal rainfall [800–2,400 mm/yr (11)]. Lowland vegetation is dominated by wet Zambezian woodlands, replaced by evergreen and then montane forests with increasing elevation (12). Lake Malawi itself is hydrologically open, drained by the Shire River, although 82% of total water loss is through evaporation (13). It is currently a dilute (240–250 μS/cm conductivity), stratified water body, with negligible nutrient concentrations in surface waters, leading to very high water clarity (14).

In 2005, we collected drill cores from two sites in Lake Malawi (15, 16). The deep-water central basin, site 1 (11°17.66′S, 34°26.15′E, 592 m water depth) was drilled to provide a relatively complete record even during extreme low-lake stands. Four cores were retrieved from this site, one of which (MAL05-1C, 76 m in length) forms the basis for this study. The north basin, site 2 (10°01.06′S, 34°11.16′E, 361 m) was located where earlier studies (4) had shown the potential for a high-resolution record covering the last ≈100 ka. Seismic data indicating deep-water unconformities and low-stand deltas, plus total organic carbon/total inorganic carbon, saturated bulk density, and faunal data from the deeper site, yield a coherent record of extremely low lake levels (−550 to −600 m relative to modern water depths) from ≈135 to 127 ka, and again from 115 to 95 ka, with lake levels rising in a stepped and sometimes reversing fashion thereafter and reaching near-modern levels ≈60 ka (16). This occurrence of unprecedented megadroughts was manifested as well in our shallower drill site in Lake Malawi and in long core records from Lake Tanganyika and from Lake Bosumtwi in West Africa (16). In contrast to the extreme low lake levels experienced in the early Late Pleistocene, the aridity of the LGM appears to have been much less severe, with lake levels on the order of 30–200 m below modern from ≈35 to 15 ka (17). The present study demonstrates the profound ecological consequences of these extreme drought intervals and discusses their implications for both lacustrine species flock evolution and anatomically modern human demography and expansion out of Africa.

Results

Screen-Washed Samples (Fig. 1). *Ostracodes.* Low-diversity ostracode assemblages were found in several intervals of core 1C before 62 ka. All of these assemblages are exclusively benthic/epibenthic taxa that cannot survive under conditions of sustained lake floor anoxia, a condition that currently exists in Lake Malawi in water depths >200–250 m (14). Fossil transport from a shallower water source to deep water can be discounted, given the extreme fragility of the ostracode fossils and because the anoxic part of the lake is under-

Author contributions: A.S.C., K.R.M.B., C.A.S., T.C.J., J.W.K., and M.R.T. designed research; A.S.C., J.R.S., K.R.M.B., L.E.P., P.N.R., D.D., C.A.S., T.C.J., J.W.K., M.R.T., E.T.B., and S.J.I. performed research; A.S.C., J.R.S., and K.R.M.B. analyzed data; and A.S.C., J.R.S., K.R.M.B., and P.N.R. wrote the paper.

The authors declare no conflict of interest.

This article is a PNAS Direct Submission. D.H. is a guest editor invited by the Editorial Board.

Abbreviations: DCA, detrended correspondence analysis; LGM, Last Glacial Maximum; PAR, pollen accumulation rate; PCA, principal components analysis.

†To whom correspondence should be addressed. E-mail: cohen@email.arizona.edu.

This article contains supporting information online at www.pnas.org/cgi/content/full/0703873104/DC1.

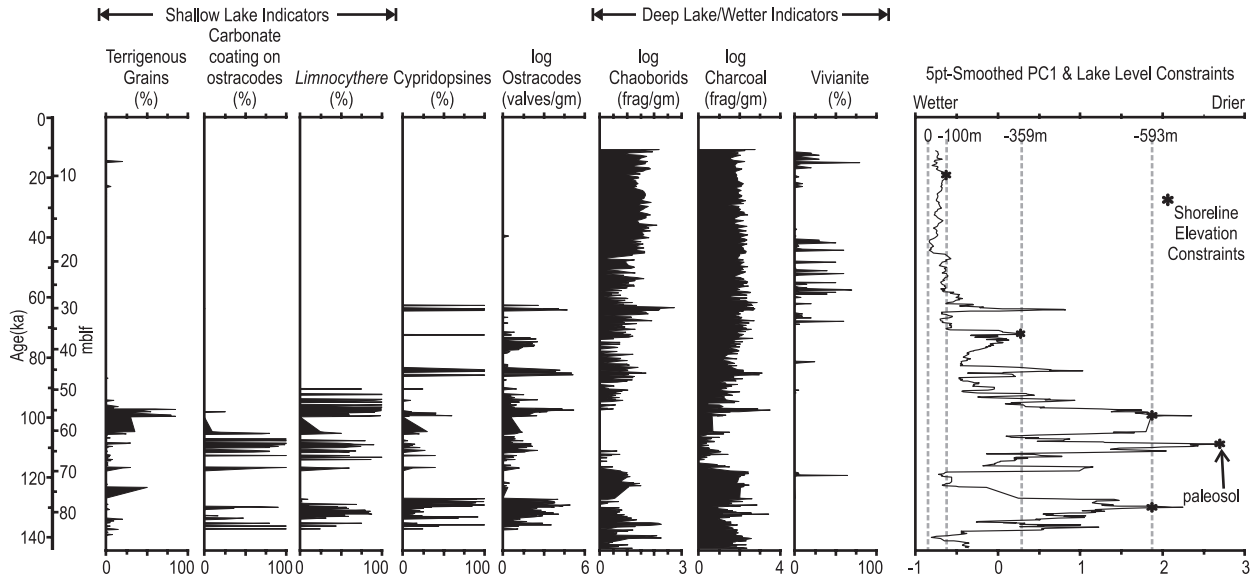

Fig. 1. Screen-wash records vs. time and depth for core 1C and PCA first axis of variance (strongly correlated with lake level) vs. time and depth. mblf, meters below lake floor. The probable paleosol at 108.5 ka indicates a minimum lake-level decline: The lake may have dropped below the core site elevation.

saturated with respect to $CaCO_3$. On the basis of maximal depths of the oxygenated zone in nearby Lake Tanganyika, which, under windy conditions, can be ventilated down to ≈250–300 m (18), we interpret the occurrence of abundant ostracodes as indicative of water depths at least ≈280 m shallower than at present. Two ostracode assemblages are particularly diagnostic:

- A saline, alkaline lake assemblage consisting of monospecific *Limnocythere* sp. (with subordinate *Candonopsis*, *Ilyocypris*, and *Sclerocypris* in some samples) (Fig. 2) typifies shallow, littoral conditions in highly alkaline (pH 9–9.5; alk >30 meq/liter) and saline (K_{20} > 4,000 μS) African lakes (19). *Limnocythere* assemblages are characterized by high adult/juvenile ratios, low levels of decalcification, common carbonate coatings, and frequent valve abrasion, all typical of reworking and accumulation in the littoral zone of a large African lake (20, 21). These assemblages occur between 133 and 130 ka and between 118 and 90 ka.
- Deeper water conditions (tens to a few hundreds of meters) are indicated by a dominance of weakly calcified, juvenile valves of endemic cypridopsine ostracodes (20) that are frequently extremely abundant and show no signs of coatings or abrasion. This assemblage occurs in transitional zones (136–133, 129–128, and 86–63 ka) between the littoral assemblage and the appearance of indicators of bottom-water anoxia. Deltaic strata preserved at the −200-m level and dated at 62–64 ka (16), coupled with a deep-water ostracode assemblage from the same time interval, demonstrate that Lake Malawi must have once been ventilated to greater depths (≈350–400 m) than at present.

Chaoborids. Chaoborid (phantom midge) larvae are extremely abundant zooplankters in open-water regions of modern Lake Malawi (22). Their pattern of fossil abundance is the inverse of the ostracodes, with either an absence or very low abundances through most of the megadrought interval and common occurrence over

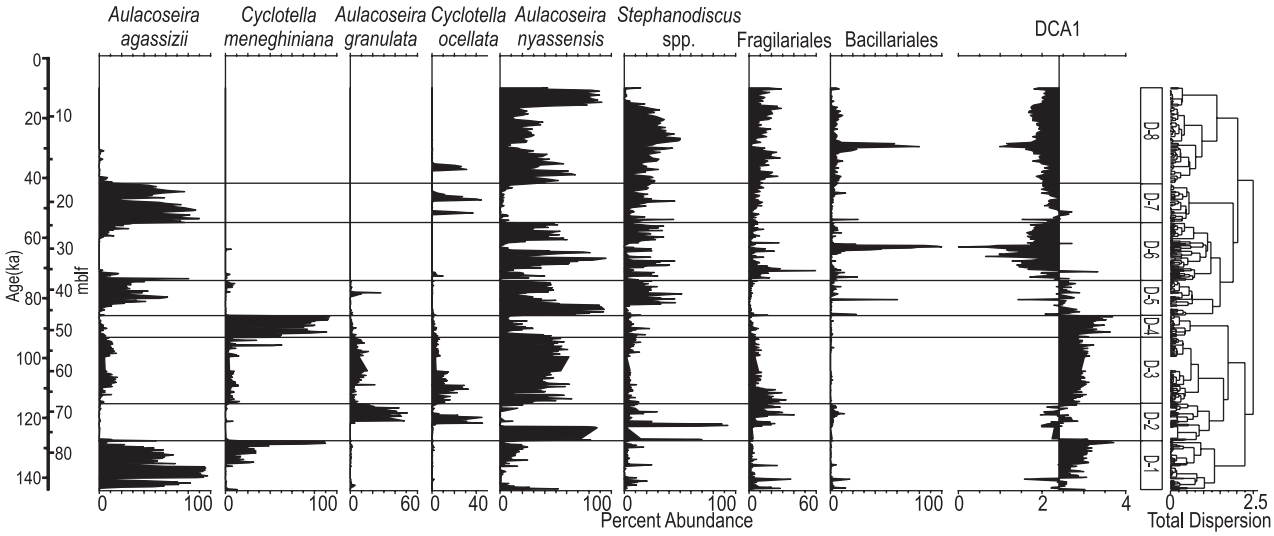

Fig. 2. Stratigraphic profile of select diatom species and taxonomic groups and DCA1. Horizontal lines indicate diatom zones from constrained cluster analysis. A dendrogram is plotted to the right of the diagram.

most of the last 60 ka. Because of their ability to take refuge from predators by vertical migration into anoxic and/or low-light, deep-water habitats (23), they are particularly abundant in stratified tropical lakes, and the abundance of their fossils is correlated with the extent of lake-floor anoxia above a core site (24).

Charred particles. Charred-particle abundance varies over four orders of magnitude in the core 1C record, providing an excellent indicator of fire frequency near the drill site. Between ≈115 and 96 ka, charcoal abundance drops to near zero (largely corresponding with the *Limnocythere* ostracode-dominated lake interval), pointing to a period of extreme aridity, when the landscape converted periodically to semidesert, with disconnected plant cover and limited fuel beds incapable of sustaining major fires. In southern Africa, the modern precipitation threshold for fire-sustaining fuel beds is ≈400 mm/yr (25), suggesting that precipitation was this low or lower during the no-charcoal phase of the megadrought. Charcoal abundance rises dramatically after 96 ka, reaching near-modern (pre-20th century) levels by ≈60 ka, with a minor drop during the LGM.

Principal components analysis (PCA). Data from PCA of screen-washed samples [see supporting information (SI) *Text* and SI Table 1 for mineralogy data] yields a coherent picture of paleoecological change at Lake Malawi over the last ≈150 ka (Fig. 1). The first PCA axis (PC1) for all analyzed variables (those displayed plus those from ostracode taphonomy results, percentage adults, percentage broken valves, and percentage whole carapaces) explains 32.3% of the data variance and contrasts strongly positive loading variables (percentage *Limnocythere* spp., percentage total ostracode abundance, percentage adult ostracodes, and percentage broken valves) with strongly negatively loading variables (chaoborid, charcoal, and vivianite abundance). These results show that PC1 is primarily a lake-level/watershed moisture availability axis, consistent with the illustrated paleolake-level constraints (16) that can be placed either on the core or on Lake Malawi itself for the last ≈150 ka. Prolonged low lake levels and aridity occurred between 105 and 95 ka, with shorter episodes at ≈111–108 ka and ≈127–132 ka. Low stands are associated with shoreline indicators that lake level had dropped at least to the core site elevation. Lesser episodes of aridity are indicated by smaller peaks after the main megadrought period ended, from 95 until ≈60 ka. In contrast, the LGM, a time of well documented aridity throughout tropical East Africa (26, 27), is manifested by only a very small rise in PC1 scores, consistent with the much smaller lake-level decline at that time.

Diatoms. Light microscopy revealed a diverse diatom assemblage, with 112 taxa enumerated. All assemblages are dominated by plankton and tychoplankton (accidental plankton) forms, and abrupt transitions in the dominant species are common (Fig. 2). Stratigraphically constrained cluster analysis quantitatively defined eight zones, which conform to major shifts in the axis of maximum variance as determined by detrended correspondence analysis (DCA) (DCA1; 13% of total variance) (see SI Tables 2 and 3). DCA1 sample scores are typically high before ≈85 ka and low after ≈74 ka.

Diatom zones D-1 to D-4 (150–85 ka). Diatom zones D-1 and D-3 are dominated by *Aulacoseira* species that are common at low abundances in modern Lake Malawi (28–30). Increased abundances of *Aulacoseira* species in the modern lake are often associated with shallower water environments and higher silicate concentrations in the water column (14, 31–33). The dominance of *Aulacoseira* species before ≈85 ka suggests that the lake was much shallower and more frequently mixed than today. Diatom zones D-1, D-3, and D-4 are characterized by the highest DCA1 scores, associated with increased abundances of *Cyclotella meneghiniana*. This taxon has never been reported as abundant in the modern flora of Lake Malawi but occurs elsewhere today in East Africa in saline or moderately alkaline, nitrogen-rich waters (34–36). In large lakes, it tends to dominate the nearshore plankton when chloride inputs are high and salinity levels fluctuate rapidly (37). The presence of this species as a common component of fossil assemblages suggests saline waters associated with drastically lower water depths.

Gradual increases in abundance of *C. meneghiniana* in the upper half of zones D-1 and D-3 suggest fluctuating salinity and low silicate concentrations associated with rising lake levels and less frequent mixing. Abundant *Stephanodiscus* species and the abrupt disappearance of *C. meneghiniana* throughout most of zone D-2 indicate deeper lake conditions than those observed in zone D-4, where *C. meneghiniana* remains the dominant form throughout and waters probably remained somewhat saline. The appearance of *Cyclotella ocellata*, a facultative plankter often considered to be littoral, at the top of zone D-2 suggests declining lake levels. Although there are no modern analogues in East Africa where *C. ocellata* is a dominant taxon, fossil assemblages rich in *C. ocellata* have been reported from Lakes Abhé and Tanganyika, where it was associated with water depths ranging from 100 to 150 m (38, 39).

Diatom zones D-5 to D-8 (85–10 ka). The upper four diatom zones differ markedly from the lower four zones, as illustrated by the negative shift in DCA1 scores. This transition coincides with the disappearance of *C. meneghiniana* and *C. ocellata* at the top of D-4, an abrupt increase in the relative abundance of *Stephanodiscus* species, and gradual increases in other species that are common in low abundances in the modern and Holocene flora of Lake Malawi (28–30). These transitions suggest a shift toward much higher lake levels. Lake levels continued to fluctuate widely throughout zones D-5 and D-6 but never fell to the levels observed in the lower four diatom zones. Zones D-7 and D-8 show a decrease in sample-to-sample variability and a gradual increase in the abundances of *Stephanodiscus* species, suggesting that lake levels continued to rise and that the stratification of the lake became more pronounced, resulting in less frequent mixing of the water column.

Palynology. Between 120 and 75 ka, the pollen record shows a predominance of grass, with diverse yet sparsely represented arboreal, herbaceous, and wetland components surrounding Lake Malawi (Fig. 3 and see SI Table 4). Pollen spectra include both deciduous and evergreen arboreal taxa (*Celtis*, *Acalypha*, and Moraceae), as well as representatives from a lowland Zambezian miombo woodland ecosystem (*Brachystegia*, *Uapaca*, *Isoberlinia*, and *Faurea*). Particularly striking is the relatively high pollen accumulation rate (PAR) values for *Podocarpus* and other montane indicators such as Ericaceae, *Olea*, *Juniperus*, and *Ilex*. Within this interval, *Podocarpus* PAR and percentages even exceed Poaceae at selected depths (35–38%), and the combined montane taxa represent an average of 20% of the grains deposited at the core site. In contrast, at no time during the last 35 ka did *Podocarpus* pollen percentages exceed 12% of the total pollen (ref. 40 and the present study). Samples from within the *Podocarpus* forest of the Drakensburg Mountains contain only ≈40% *Podocarpus* pollen (41). These data, in conjunction with our results, strongly suggest substantial expansion of montane forest taxa to lower elevations within the highlands north and west of Lake Malawi (42). Such expansion would require cooler conditions, at least seasonally. The combined pollen and charred-particle data suggest that an ecosystem similar to the high-elevation semideserts of South Africa today probably existed near the lake shore, with expanded montane forests at higher elevations (43).

The substantial changes in total PAR after 105 ka inversely mirror the terrigenous component (percentage sand fraction) of sediment, with accumulation rates falling by an order of magnitude when Lake Malawi was very shallow. Because sedimentation rates do not increase along with the increase in sand, the decline in PAR at these times probably is not due to dilution or grain degradation but instead reflects a real change in pollen productivity and/or transport to the coring site. The percentage of broken/crumpled grains remains ≈8% throughout the entire 120- to 75-ka interval.

From 105 to 95 ka, PARs fall to an average of <250 grains per

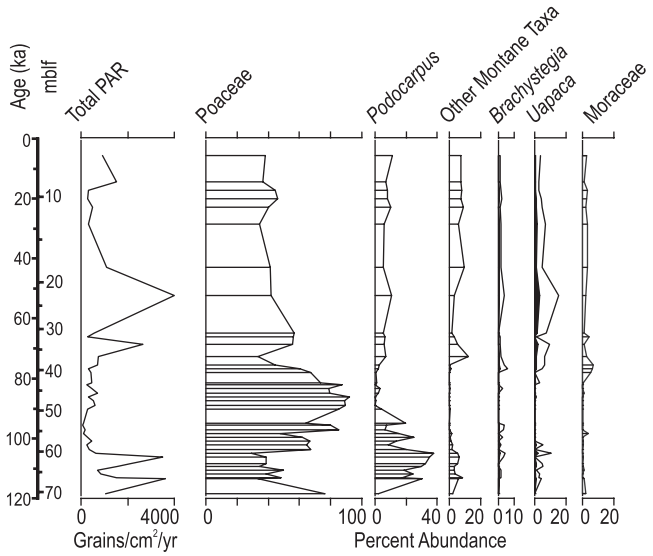

Fig. 3. Summary palynostratigraphy of core 1C. (See SI Table 4 for details and additional taxa.) Other montane taxa include *Olea*, *Kiggelaria*, *Ilex*, *Juniperus*, *Apodytes*, and *Syzygium*. *Brachystegia* and *Uapaca* plots are shown with actual percentage values and at 5× exaggeration.

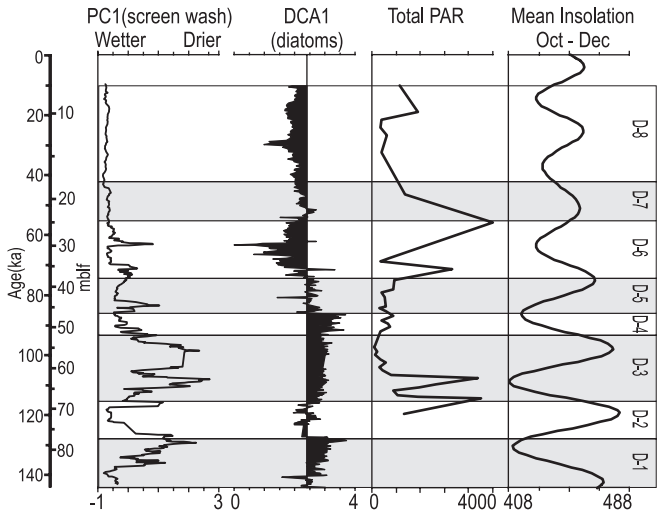

Fig. 4. Comparison of major summary paleoecological records for core 1C. From left to right: PC1 for screen-wash data, DCA1 for diatom data, total PARs, and rainy season solar insolation (W/m^2) for the drill site.

square centimeter per year. The scant pollen deposited at the coring site is increasingly dominated by Poaceae, whereas *Podocarpus*, other montane taxa, and Zambezian miombo woodland indicators like *Uapaca* diminish. The continued presence of *Brachystegia* suggests a transition to the drier miombo (rainfall <1,000 mm), in which trees are sparse and most if not all of the subdominant trees are absent (12). *Typha* pollen is found consistently within this interval, suggesting that emergent wetlands occurred along the lowered lake shore (see SI Table 4). By the end of this interval, pollen from *Brachystegia* and montane taxa is absent except for a few, potentially reworked, *Podocarpus* grains.

After ≈93 ka, PARs increase, although they remain much lower than before 105 ka, presumably reflecting post-megadrought recovery and expansion of plants. Notably, the montane taxa, as well as *Brachystegia* and pteridophytes, do not rebound. The limited deposition of montane taxa throughout the 93- to 75-ka interval suggests that extreme aridity of the megadrought extending up to high elevations may have killed off montane taxa that previously flourished. With minimal source areas nearby to "restock" the isolated mountain highland "islands," the montane communities could not reestablish immediately, despite increasing moisture as suggested by rising lake levels. During the last 70 ka, the vegetation within the Lake Malawi pollen source area remains fairly consistent with diverse lowland and montane plant communities. Notable is the lack of any substantial shift in plant types during the LGM.

Discussion

In sum, our findings demonstrate that the Lake Malawi region experienced extreme aridity episodically between 135 and 70 ka, with diminished climatic and ecologic variability after 70 ka. Patterns of variability are broadly consistent between terrestrial and lake paleoecologic changes and are also consistent with precessional forcing for the drill site (ref. 16 and Fig. 4). During the most arid intervals, Lake Malawi became a shallow alkaline, saline lake, with lake levels at least as low as −580 m, and its surrounding watershed was converted into a semidesert. In conjunction with previous studies (16, 44–46), these results document a wide-ranging, tropical African event of broad ecological significance. Furthermore, our continuous and regionally significant record of aridity during this period shows it to have been much more severe than during the LGM, a period assigned great importance in hypotheses regarding the impacts of aridity on African ecosystems and evolution (3, 47). Although LGM aridity is clearly demonstrable throughout tropical Africa, our findings suggest that its impact on lake and terrestrial ecosystems would have been less than that of the preceding early Late Pleistocene megadroughts.

Unlike the smaller lake-level falls suggested for the LGM (27), the early Late Pleistocene conversion of Lake Malawi to a relatively shallow lake would have eliminated most rocky shoreline habitat in the lake, leaving the majority of the lake's shoreline with a muddy or sandy bottom. This alters our understanding of the physical setting for evolution of the lake's endemic fauna. The estimated 500–1,500 species of cichlid fishes in Lake Malawi are intensively studied as model systems for speciation, with sexual selection based on visual mate choice as a preferred hypothesis for the elevated diversity (48). A shallow and probably turbid, well mixed lake with reduced visibility (as suggested by the diatom flora) might impede cichlid mate choice and negatively impact species maintenance and coexistence (49). These conditions could have significantly affected the rocky-dwelling littoral cichlid communities (*mbuna*) that currently account for 20–50% of the extraordinary diversity of the lake's cichlids. Simultaneous lake-level falls at nearby Lake Tanganyika during both the megadrought [on the order of 400–600 m (16, 50)] and the LGM (100–250 m) would not have had as great an impact on the extent of rocky habitat required for its endemic littoral fauna, or on water chemistry, given the much greater depth and volume of that lake (see *SI Text* and SI Fig. 5 for further discussion).

Prior attempts to date major diversification events within the cichlids (47, 51–53) have been based on the timing of the post-LGM lake-level rise and on much older, weakly constrained outcrop (54) or seismic data (55, 56) from the two lakes. The megadrought low-stand demonstrated here for Lake Malawi provides a much more robust constraint on genetic divergence within the cichlid phylogeny, implying rates of evolution four to eight times slower than those that assume a major role for the LGM in Lake Malawi speciation. Conversely, the most recent megadrought is much younger than nuclear (57) or mitochondrial (47) molecular clock estimates of mbuna and non-mbuna cichlid divergence (0.7 ma and 0.57–1.0 ma, respectively). Our results also suggest that the concept of synchronous cichlid diversification events in the three largest African lakes (Malawi, Tanganyika, and Victoria) bears reconsid-

eration given their probable different responses to the megadrought (Tanganyika 800–1,000 m deep, moderately saline, extensive rocky coastal habitat assuming a near-modern basin configuration, possibly subdivided into multiple basins; Malawi, 100 m deep and saline, little rocky habitat, subdivided at times; Victoria, no record but probably dry) and the LGM arid phase [Malawi and Tanganyika, closed and undivided deep basins with abundant rocky habitat; Victoria, dry (27)] (see *SI Text* and SI Fig. 5 for further discussion).

Our terrestrial ecological record, when coupled with other regional records of widespread southern tropical African aridity during the megadrought interval, has additional implications for early Late Pleistocene human demography and archaeology in Africa. The Lake Malawi record shows a shift from a period of high-amplitude climate variability between 140 and 70 ka, with at least two distinct episodes of desert-like conditions in tropical Africa, followed by a period of lowered variability over the last 70 ka, with generally more humid climates throughout that period, including the somewhat arid LGM (16). Whereas extreme variability in African climate regimes before 70 ka has been reported elsewhere in subSaharan Africa, it has primarily been in the context of unusually wet conditions [e.g., dated high stand deposits in the Kenyan rift (6)], in contrast to our evidence for extreme aridity. This interregional variability will make it difficult to identify specific region(s) (e.g., centers of modern forests) as persistent Afrotropical refugia throughout the Middle/Late Pleistocene. More likely, refugia themselves migrated in parallel with the intense climate swings, consistent with genetic evidence for chimpanzees (58). In this regard it is noteworthy that, simultaneous with the peak period of tropical African aridity [recorded at Lakes Malawi, Tanganyika, and Bosumtwi (16) and in the records of expanding deserts and active dune fields in both West Africa and the northern Kalahari (44–46)], abundant evidence exists for human occupation in southern and northern Africa, as well as in the Levant, whereas directly dated sites in tropical Africa are rare (59–62). The long African lake core records also make it less likely that the period of minimal human populations in equatorial Africa can be linked to events occurring after 80 ka (63). Furthermore, we propose that the expansion of more humid climate biomes is consistent with most models of both human and chimpanzee population expansion (64–67). The end of arid conditions in tropical Africa closely coincides with the onset of aridity elsewhere on the continent and in the Levant (9, 68, 69). Thus, a likely period for human population expansion out of equatorial Africa (especially up a Nilotic corridor from tropical to North Africa) would have been during the climatic "crossover" time, between ≈90 and 70 ka, when intermediate precipitation regimes would have prevailed throughout Africa. This interval is long enough to accommodate a zone of contiguous habitability during a genetic "sweep" up the Nile (65) and early enough to accommodate even early proposed arrivals of humans into Australia (70). It is also consistent with the idea (71) that the earlier (≈125 ka) documented occurrence of modern humans in North Africa and the Levant represents ultimately unsuccessful "excursions" out of Africa.

Methods

Core collection, geochronology, and archiving are described elsewhere (15, 16). After splitting, core MAL05-1C was sampled at 16-cm intervals (≈300-yr resolution) for screen-wash and diatom analysis and at 1-m intervals for pollen samples. In total, 467 samples were collected for screen-wash and diatom analysis and 40 for palynology.

Screen-Washed Samples. Weighed wet sediment samples were disaggregated in deionized water and sieved using a 125-μm stainless steel sieve. Wet weights were determined for a separate aliquot from each sample, which was oven-dried and reweighed to determine water content and to calculate original dry weights for sieved samples. After sieving, residues were counted at 90× for ostracodes [total number per sample, taphonomic condition (percentage adult, broken, carbonate coated, and reduction/oxidation stained), percentage major genera based on 100 valve counts, charred particles (total abundance per sample), chaoborid fragments, and percentage mineralogy in sand fraction]. Fossil identifications were confirmed by using a Philips (Eindhoven, The Netherlands) XL30 environmental scanning electron microscope. Fossil abundance, taphonomic, and mineralogic data from the screen-wash fractions were analyzed by PCA using CANOCO 4.5 (72). First axis PCA scores were smoothed by using a five-point running average of stratigraphically adjacent samples.

Diatoms. Diatom samples were prepared from all samples for light microscope analysis by using standard sample digestion, extraction, and mounting techniques (73). Clay-rich samples were immersed briefly (15–30 s) in an ultrasonic water-bath to disaggregate the sample and allow for complete digestion. When possible, a minimum of 300 diatom valves was identified from each sample interval; highly dissolved or sparse samples with <100 diatom valves counted were excluded from statistical analyses, leaving 463 samples.

Diatom percentage abundance data were screened to remove species that did not occur in abundances of at least 1% in two samples. After the screening, percentage abundance data for the remaining 51 diatom species were square-root transformed and analyzed by stratigraphically constrained cluster analysis (CONISS) using PSIMPOLL 4.10 (74) and by DCA using CANOCO 4.5 (72).

Palynology. Sediment samples (0.5 cm^3) were processed for pollen, in accordance with standard methods (75). Before final dehydration, a calibrated micropolystyrene spike was added to each sample to allow calculation of pollen concentrations (76). For each sample, 600 identifiable grains were counted. Identified grains were grouped into vegetation types on the basis of habitat preference of the parent plant. PARs were determined as number of grains per square centimeter per year, using mean pollen concentrations and the combined depth–age model.

We thank the University of Rhode Island and Lengeek Vessel Engineering, Inc., for general contracting and barge modifications during the Lake Malawi Scientific Drilling Project; the marine operations and drilling crews of the drilling vessel *Viphya*, provided by ADPS Ltd. and Seacore Ltd., respectively; DOSECC, Inc., Malawi Department of Surveys, Malawi Lake Services, and A. E. Oberem for logistical support; the scientific participants for field operations; the government of Malawi for permission to undertake this research; D. Gauggler, R. Markus, and L. Brooke McDonough for help with sample preparation; K. Behrensmeyer, A. Brooks, E. Michel, J. Todd, C. Tryon, D. Verschuren, C. Labandeira, and P. Wigand for valuable discussions; and two anonymous reviewers for many helpful comments. Funding for the field program was provided by the U.S. National Science Foundation–Earth System History Program and the International Continental Scientific Drilling Program, with additional funding for A.S.C. from the Smithsonian Institution (Evolution of Terrestrial Ecosystems Program and Fellowship Program). Initial core processing was carried out at LacCore, the National Lake Core Repository at the University of Minnesota.

1. Fjeldsaå J, Lovett JC (1997) *Biodivers Conserv* 6:325–346.
2. Linder HP (2001) *J Biogeogr* 28:169–182.
3. Jolly D, Taylor D, Marchant R, Hamilton A, Bonnefille R, Buchet G, Riollet G (1997) *J Biogeogr* 24:492–512.
4. Johnson TC, Brown ET, McManus J, Barry S, Barker P, Gasse F (2002) *Science* 296:113–132.
5. Talbot MR, Johannessen T (1992) *Earth Planet Sci Lett* 110:23–37.
6. Trauth MH, Maslin MA, Deino A, Strecker MR (2005) *Science* 309:2051–2053.
7. Cerling TE, Harris JM, MacFadden BJ, Leakey MG, Quade J, Eisenmann V, Ehleringer JR (1997) *Nature* 389:153–158.
8. Dupont LM, Jahns S, Marret F, Ning S (2000) *Palaeogeogr Palaeoclimatol Palaeoecol* 155:95–122.

9. DeMenocal PB (2004) *Earth Planet Sci Lett*, 220:3–24.
10. Potts R (1998) *Yearb Phys Anthropol* 41:93–136.
11. Malawi Department of Surveys (1983) *National Atlas of Malawi* (Blantyre, Malawi).
12. White F (1983) *The Vegetation of Africa* (UNESCO, Paris).
13. Owen RB, Crossley R, Johnson TC, Tweddle D, Kornfield I, Davison S, Eccles DH, Engstrom DE (1990) *Proc R Soc London Ser B* 240:519–533.
14. Patterson G, Kachinjika O (1995) in *The Fishery Potential and Productivity of the Pelagic Zone of Lake Malawi/Niassa*, ed Menz A (Natl Resources Inst, Chatham, UK), pp 1–67.
15. Scholz CA, Cohen AS, Johnson TC, King JW, Moran K (2006) *Sci Drilling* 2:17–19.
16. Scholz CA, Johnson TC, Cohen AS, King JW, Peck JA, Overpeck JT, Talbot MR, Brown ET, Kalindekafe L, Amoako PYO, *et al.* (2007) *Proc Natl Acad Sci USA* 104:16416–16421.
17. Barker P, Gasse F (2003) *Quat Sci Rev* 22:823–837.
18. Plisnier P-D, Chitamwebwa D, Mwape L, Tschibangu K, Langenberg VT, Coenen E (1999) *Hydrobiologia* 407:45–58.
19. Cohen AS, Dussinger R, Richardson J (1983) *Palaeogeogr Palaeoclimatol Palaeoecol* 43:129–151.
20. Palacios-Fest MR, Alin SR, Cohen AS, Tanner B, Heuser H (2005) *J Paleolimnol* 34:51–71.
21. Park LE, Cohen AS, Martens K, Bralek R (2003) *J Paleolimnol* 30:127–138.
22. Irvine K (1995) in *The Fishery Potential and Productivity of the Pelagic Zone of Lake Malawi/Niassa*, ed Menz A (Natl Resources Inst, Chatham, UK), pp 109–140.
23. Rine HE, Kesler DH (2001) *J Freshwater Ecol* 16:145–150.
24. Rumes B, Eggermont H, Verschuren D (2005) *Hydrobiologia* 542:297–314.
25. Bird M, Veenendaal E, Lloyd J (2004) *Global Change Biol* 10:342–349.
26. Bonnefille R, Chalie F (2000) *Global Planet Change*, 26:25–50.
27. Johnson TC, Scholz CA, Talbot MR, Kelts K, Ricketts RD, Ngobi G, Beuning K, Ssemmanda I, McGill JW (1996) *Science*, 273:1091–1093.
28. Hecky RE, Kling HJ (1987) *Arch Hydrobiol* 25:197–228.
29. Haberyran KA, Mhone OK (1991) *Hydrobiologia* 215:175–188.
30. Gasse F, Barker P, Johnson T (2002) in *The East African Great Lakes: Limnology, Palaeolimnology, and Biodiversity*, eds Odada EO, Olago DO (Kluwer, The Netherlands), pp 393–414.
31. Owen RB, Crossley R (1992) *J Paleolimnol* 7:55–71.
32. Kilham P, Kilham SS, Hecky RE (1986) *Limnol Oceanogr* 31:1169–1181.
33. Pilskaln CH, Johnson TC (1991) *Limnol Oceanogr* 36:544–557.
34. Blin DW (1993) *Ecology* 74:1246–1263.
35. Fritz SC, Cumming BF, Gasse F, Laird KR (1999) in *The Diatoms: Applications to Environmental and Earth Sciences*, eds Stoermer EF, Smol JP (Univ Press, London), pp 41–72.
36. Gasse F (1986) *East African Diatoms: Taxonomy, Ecological Distribution* (Cramer, Berlin), Bibliotheca Diatomologica, Vol. 11.
37. Tuchman ML, Theriot E, Stoermer EF (1984) *Arch Protistenkd* 128:319–332.
38. Gasse F, Ledée V, Massault M, Fontes JC (1989) *Nature* 342:57–59.
39. Gasse F, Street FA (1978) *Palaeogeogr Palaeoclimatol Palaeoecol* 24:279–325.
40. DeBusk GH (1994) PhD thesis (Duke Univ, Durham, NC).
41. Scott L (1989) *S Afr J Bot* 55:107–116.
42. Meadows ME (1984) *J Biogeogr* 11:209–222.
43. Scott L (1982) *Quat Res* 17:339–370.
44. Nichol JE (1999) *Geogr J* 167:79–89.
45. Thomas DS, Shaw PA (2003) *Quat Sci Rev* 21:783–797.
46. Pokras EM, Mix AC (1987) *Nature* 326:486–487.
47. Sturmbauer C, Baric S, Salzburger W, Rüber L, Verheyen E (2001) *Mol Bio Evol* 18:144–154.
48. Kocher TD (2004) *Nat Rev Genet* 5:288–298.
49. Seehausen O, van Alphen JJ, Witte F (1997) *Science* 277:1808–1811.
50. Scholz CA, King JW, Ellis GS, Swart PK, Stager C, Colman SM (2003) *J Paleolimnol* 30:139–150.
51. Danley PD, Kocher TD (2001) *Mol Ecol* 10:1075–1086.
52. Sturmbauer C, Hainz U, Baric S, Verheyen E, Salzburger W (2003) *Hydrobiologia* 500:51–64.
53. Duftner N, Koblmüller S, Sturmbauer C (2005) *J Mol Evol* 60:277–289.
54. Delvaux D (1995) in *Annual Report of the Department of Geology and Minerals, 1993–1994* (Royal Museum for Central Africa, Tervuren, Belgium), pp 99–108.
55. Scholz CA, Rosendahl B (1988) *Science* 240:1645–1648.
56. Cohen AS, Lezzar KE, Tiercelin J-J, Soreghan MR (1997) *Basin Res* 9:107–132.
57. Won Y, Wang Y, Sivasundar A, Raincrow J, Hey J (2006) *Mol Biol Evol* 23:828–837.
58. Goldberg TL (1998) *Intl J Primatol* 19:237–254.
59. McBrearty S, Brooks AS (2000) *J Hum Evol* 39:453–563.
60. Walter RC, Buffler RT, Bruggemann JH, Guillaume MM, Berhe SM, Negassi B, Libsekal Y, Cheng H, Edwards L, von Cosel R, *et al.* (2000) *Nature* 405:65–69.
61. Stringer C (2003) *Nature* 423:692–695.
62. Grün R, Stringer C, McDermott F, Nathan R, Poral N, Robertson S, Taylor L, Mortimer G, Eggins S, McCulloch M (2005) *J Hum Evol* 49:316–334.
63. Ambrose SH (1998) *J Hum Evol* 34:623–651.
64. Rogers AR (2000) *Evolution (Lawrence, Kans)* 49:608–615.
65. Harpending H, Rogers A (2000) *Annu Rev Genomics Hum Genet* 1:361–385.
66. Eswaran V, Harpending H, Rogers AR (2005) *J Hum Evol* 49:1–18.
67. Goldberg TL (1996) PhD thesis (Harvard Univ, Cambridge, MA).
68. Jacobs Z, Duller GAT, Wintle AG, Henshilwood CS (2006) *J Hum Evol* 51:255–273.
69. Tchernov A (1998) in *Neandertals and Modern Humans in Western Asia*, eds Akazawa T, Aoki K, Bar-Yosef O (Plenum, New York), pp 77–90.
70. Thorne A, Grün R, Mortimer G, Spooner NA, Simpson JJ, McCulloch M, Taylor L, Curnoe D (1999) *J Hum Evol* 36:591–612.
71. Klein R (1999) *The Human Career* (Univ Chicago Press, Chicago).
72. ter Braak C, Smilauer P (2002) CANOCO 4.5 (Microcomputer Power, Ithaca, NY).
73. Battarbee RW (1986) in *Handbook of Holocene Palaeoecology and Palaeohydrology*, ed Berglund B (Wiley, New York), pp 527–570.
74. Bennett KD (2007) *Manual for* psimpoll and pscomb *Programs for Plotting and Analysis* (Queen's Univ, Belfast, Northern Ireland). Available at www.chrono.qub.ac.uk/psimpoll/psimpoll.html.
75. Faegri K, Iversen J (1989) *Textbook of Pollen Analysis* (Wiley, Chichester, UK).
76. Maher L (1981) *Rev Palaeobot Palynol* 32:153–191.

Supporting Information for Cohen et al. "Ecological Consequences of Early Late-Pleistocene Megadroughts in Tropical Africa"

Geochronology.

Geochronologic methods used to date Core MAL05-1C are discussed in detail elsewhere (1). Briefly, the age model is constrained by a series of 16 AMS ^{14}C dates on bulk organic matter in lake mud and calibrated to calendar year using CALPAL. Beyond the range of radiocarbon, the age model is constrained by 6 paleointensity/^{10}Be correlations, 1 magnetic inclination date and 2 OSL dates. The 0-50ka interval depth (meters below lake floor-MBLF)/age relationship was fit to a 3rd order best fit polynomial (Age= -4.35595(MBLF^3)+176.1671(MBLF^2)+611.8615(MBLF), whereas the older portion of the record (where the relationship was not as well constrained) was fit to a best-fit linear age model (Age=1360.059(MBLF)+22728.51).

Screen Wash Mineralogy.

Vivianite $Fe_3(PO_4)_2$-$(H_2O)_8$ crystal clusters occur episodically in Core 1C sediments. The reduced iron and phosphate required for this mineral's formation suggest its occurrence is linked to their availability in bottom or pore waters. Crystals within the clusters are randomly oriented, indicating formation at or close to the sediment/water interface (2). In modern Lake Malawi, such conditions are met only below the oxycline, where both a lack of surface mixing and nutrient uptake by phytoplankton occur. Vivianite is found forming commonly today in Lake Malawi and elsewhere in East African lakes under reducing conditions (3,4). Vivianite formed abundantly at the core site after about 68ka, indicating sustained meromixis, except for a probable hiatus during the LGM.

Terrigenous sand abundance (Q+F+L) displays a near-inverse pattern to vivianite. Where sands are abundant they occur in cm-dm scale, ungraded and mottled beds. They show deep burrowing and bedding features typical of shallow-water deposition.

Conceptual model of the impact of lake level fluctuations on Lakes Malawi, Tanganyika and Victoria (Supporting Documents Figure 1).

Vertically exaggerated cross sections and distribution of generalized substrate conditions from the three lakes are shown across the deepest parts of each lake. For Lake Malawi, this is an E-W section at 11°12S, slightly north of the core site. For Lake Tanganyika, this is an E-W section at 7°30S, and for Lake Victoria, this is a NW-SE section starting from the western shore at the equator. Note the major differences in proportions of different substrate types and limnological conditions that would have resulted from simultaneous events in the three lake basins during the Last Glacial Maximum and the Megadought intervals. Today both Lakes Malawi and Tanganyika are strongly stratified, with extensive rocky bottom habitat lying within the oxygenated portions of the water column (6). In both lakes the extent of rocky habitat is strongly correlated with the occurrence of major border faults, and rocky coastlines alternate with sandy/muddy regions along the shoaling margins of the half-graben basins (7) Both lakes also display exceptional water clarity, important for the sexual selection models based on mate color choice invoked for many endemic cichlid

fish species (8). Lake Victoria, which also has rocky habitats both on its margins and on the shores of many islands, is much shallower than the other two lakes. It has become stratified since the mid-20th Century, probably largely the result of recent climate change in the region and water column warming (9). It has also undergone cultural eutrophication over the same time period, resulting in a considerable decline in water clarity, with probable deleterious implications for its large number of haplochromine cichlid fish species, which rely on visual cues of coloration for breeding (10).

Different environmental conditions prevailed in the three lakes during the Last Glacial Maximum (LGM). All three lake basin experienced more arid and cooler conditions than at present (11,12,13). Lake Victoria was completely or nearly dry during this time period, whereas variable, but considerable lake-level falls occurred in Lakes Malawi and Tanganyika as shown. However, because of the steep, rift margins of the two lakes, and because of their great depths, both would have retained extensive rocky habitat during the LGM as indicated. Mixing depths are known to have been deeper in Lake Tanganyika during the LGM based on bioturbation of LGM-aged sediments currently at ~600m water depth, indicating mixing to at least ~350m depth during the LGM. No comparable constraints are available for Lake Malawi for this time. During the Early Late Pleistocene Megadroughts, lake level falls of at least 600m for Lake Malawi and ~400-600m for Lake Tanganyika occurred. The resulting effect would have been to reduce rocky habitat for cichlids to a relatively small region of the west coastline of the reduced lake, whereas in Lake Tanganyika, because of its much greater depth, the same lake level fall would leave extensive, though discontinuous rocky coastlines around much of the basin. Furthermore, the diatom paleoecological data indicates that the lake water turbidity would have likely been much higher at this time in Lake Malawi. The analogous evidence for rampant hybridization and loss of species diversity in modern Lake Victoria for haplochromine cichlids under similar circumstances (10) suggests that a diverse cichlid fauna reliant on visual cues for mate recognition is unlikely to have persisted in Lake Malawi during this time period.

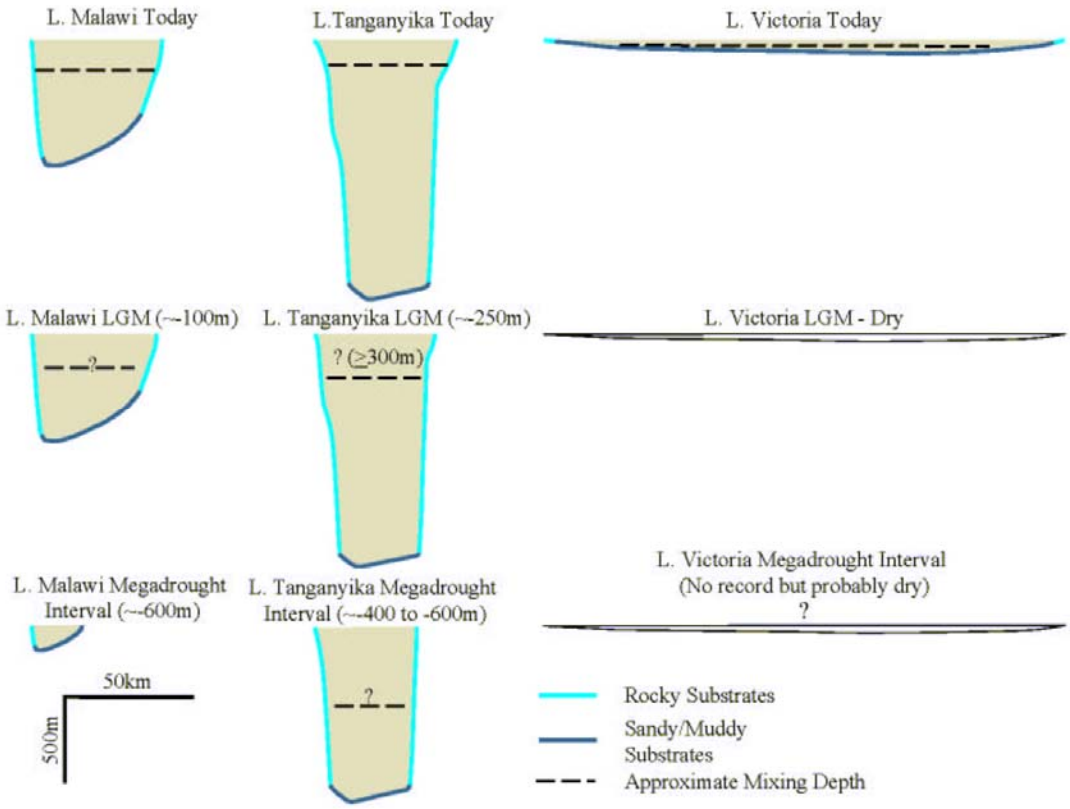

Supplemental Documents Figure 1. Conceptual model of the impact of lake level fluctuations on Lakes Malawi, Tanganyika and Victoria. Lakes are shown in vertically-exaggerated cross sectional bathymetric profiles through their deepest points today, and at the same positions during the Last Glacial Maximum (LGM) and at the height of the Early Late Pleistocene megadrought. Substrates shown are for the position of the profile only. Dashed line for approximate mixing depths indicates the average extent of oxygenated water below the surface inhabitable by animals.

Supporting Documents Table 1. Multivariate Analyses of Screen-Wash Data. Screen wash data included a variety of data types, making it preferable to analyze this information using a Principal Components Analysis. First axis loadings are discussed in the text. Slightly over 32% of the variance is explained by this axis, which we interpret, based on the loadings as being fundamentally related to lake level and available moisture (high positive loadings correlate with low lake levels and aridity).

Scores from Principle Component Analysis of Malawi Core 1C				
Eigenvalue	**0.3229**	**0.1661**	**0.1081**	**0.0877**
Item	**Axis 1**	**Axis 2**	**Axis 3**	**Axis 4**
Cypridopsines (%)	0.4888	-0.667	0.1628	-0.0098
***Limnocythere* (%)**	0.6851	0.125	-0.1221	0.11
Ostracode Adults (%)	0.6711	0.3124	0.4371	-0.0688
Broken Ostracodes (%)	0.7354	-0.551	-0.0413	0.0666
Ostracode Carapaces (%)	0.4876	0.4217	0.4843	-0.0821
Carbonate coating on ostracodes (%)	0.6636	0.3344	0.2207	-0.0479
Vivianite (%)	-0.2072	0.0613	0.2451	0.9327
Terrigenous Grains (%)	0.4454	0.2176	-0.046	0.1327
log Ostracodes (valves/gm)	0.6923	-0.5857	-0.0718	0.0571
log Charcoal (fragments/gm)	-0.4702	-0.4877	0.477	0.015
log Chaoborids (fragments/gm)	-0.4822	-0.2082	0.6141	-0.2074

Supporting Documents Table 2. Diatom Cluster Analysis

The manuscript text highlights 8 major diatom zones, based on stratigraphically-constrained cluster analysis of the major diatom taxa. The final seven stages of cluster merging involve only the merging of the clusters associated with these 8 zones. Cluster merges were analyzed using the Broken Stick Method; this technique analyzes the increase in dispersion (variance) of the cluster at each stage in the merge to determine whether the increase in dispersion associated with the addition the new cluster is significant (5). The final seven cluster merges were determined to be significant by this method.

Diatom Sample Cluster Analysis - Broken Stick Method					
Taxa	**Levels**	**Dissimilarity Coefficient**			**Transformations**
51	463	Edwards & Cavalli-Sforza's Chord Distance			Square Root
Stage Merged	**Clusters Merged**		**Increase in Dispersion**	**Total Dispersion**	**Within-Cluster Dispersion**
456	D5	D6	976.41	14520.73	6292.51
457	D2	D3	984.68	15505.41	3861.82
458	D4	D2-3	1363.42	16868.83	5590.91
459	D7	D5-6	1526.47	18395.30	8374.31
460	D8	D5-7	1327.19	19722.49	11750.89
461	D1	D2-4	2120.12	21842.61	10091.71

462	D1-4	D5-8	2389.90	24232.50	24232.50

Supporting Documents Table 3. Detrended Correspondence Analyses of Diatom Data. Detrended Correspondence Analysis was run on 51 major diatom species from diatom samples of Core MAL05-1C. First axis loadings (DCA1) are discussed in the text. Approximately 13% of the total variance is explained by this axis. Diatom taxa with the highest loadings of DCA1 commonly occur in samples prior to ~85ka and are associated with fluctuating salinity, shallower-than-modern water depths, or high silicate concentrations in the water column resulting from increased mixing. Species scores of diatom taxa analyzed are shown below, including the first four DCA axes.

Diatom species scores from Detrended Correspondence Analysis of Malawi Core 1C				
Eigenvalue	**0.2977**	**0.1858**	**0.1441**	**0.1125**
Taxon	**DCA 1**	**DCA 2**	**DCA 3**	**DCA 4**
***Aulacoseira nyassensis* B (OMüller) Simon**	2.2242	1.574	0.1892	0.6564
Stephanodiscus* cf. *medius	2.5286	1.7877	1.4664	1.1895
***Aulacoseira nyassensis* A (OMüller) Simon**	3.153	0.2497	1.168	0.3365
***Fragilaria africana* Hustedt**	2.3294	0.4095	1.0849	1.6742
Fragilaria* cf. *lancettula	2.053	0.8042	1.3468	2.1002
***Aulacoseira agassizii* (Ostenfeld) Simonsen**	3.2385	2.8965	2.551	1.5545
***Stephanodiscus nyassae* Klee et Casper**	1.1864	1.5485	1.0742	1.2862
***Aulacoseira ambigua* (Grunow) O. Müller**	3.3351	0	2.0356	0
***Cyclotella meneghiniana* Kützing**	4.3556	1.1363	1.8259	1.0944
***Cyclotella ocellata* Pantocsek**	3.6653	-0.4612	0.4866	2.4133
***Cocconeis neothumensis* Krammer**	1.4007	1.033	1.6577	2.619
***Aulacoseira granulata* (Ehrenberg) Simonsen**	3.7044	-0.7006	0.7333	2.8512
Navicula* cf. *lapidosa	1.3679	1.3163	1.7264	2.4601
***Nitzschia epiphytica* O. Müller**	0.9958	1.1779	2.0818	1.4554
***Stephanodiscus mulleri* Klee & Casper**	1.8427	-0.0487	1.7412	2.342
***Pseudostaurosira brevistriata* (Grunow) Williams & Round**	1.7703	0.3396	1.106	2.874
***Staurosirella pinnata* (Ehrenberg) Williams et Round**	1.4264	0.2871	1.8933	2.6074
***Cyclostephanos malawiensis* Casper and Klee**	2.8792	2.0289	2.9328	3.7474
***Navicula seminuloides* Hustedt**	1.1527	1.4262	1.5821	2.7716
***Cyclostephanos damasii* (Hustedt) E.F. Stoermer & H. Håkansson**	3.772	-1.7	0.2238	2.1697
***Amphora pediculus* (Kützing) Grunow**	1.1831	1.2579	1.9645	2.8849
***Cavinula scutelloides* (Smith) Lange-Bertalot et Metzeltin**	2.1011	1.4749	1.9163	1.3409
***Aulacoseira nyassensis* C (OMüller) Simon**	0.8099	1.5778	-0.1052	1.0263
***Stephanodiscus* sp. 1 Malawi**	3.9499	1.3828	0.5705	2.6797
***Nitzschia nyassensis* O. Müller**	-0.5577	0.9806	3.6391	0.9036
***Discostella stelligera* (Hustedt) Houk et Klee**	3.7291	1.9554	2.6643	2.8132
Cycolotella* cf. *distinguenda	-0.0124	2.3065	-0.6668	-0.0236
***Nitzschia latens*? Hustedt**	0.5392	0.5776	4.3769	-0.2958
Rhopalodia* cf. *gracilis	0.6756	0.6838	1.624	2.4779
***Nitzschia lancettula* O. Müller**	0.9877	0.1494	2.7132	1.9701
***Fragilariforma hungarica* (Pantocsek) PB Hamilton**	2.8671	0.5109	1.2907	2.6262
***Aulacoseira granulata* m. *curvata* (Ehrenberg) Simonsen**	1.2519	-0.0846	3.2855	-0.3976
***Thalassiosira* sp. Malawi**	2.6951	0.1826	3.7206	-1.376
***Planothidium rostratum* (Østrup) Lange-Bertalot**	1.4271	0.4475	2.0476	3.0352
***Nitzschia frustulum* (Kützing) Grunow**	2.3971	-0.2954	2.5782	4.8296
***Nitzschia lacuum* Lange-Bertalot**	0.6541	0.2692	4.0405	0.0085
***Staurosira construens* v. *construens* Ehrenberg**	1.2668	0.7198	1.704	0.8556
***Navicula radiosa* v. *parva* Wallace**	1.273	2.7045	2.7559	3.2397
***Placoneis gastrum* (Ehrenberg) Mereschkowsky**	1.0091	0.72	2.661	3.0499
***Cymbellonitzschia minima* Hustedt**	1.5211	-0.1598	1.7166	2.7029
***Stephanodiscus* sp. 2 Malawi**	3.1024	2.0577	0.0049	0.3835
***Karayevia clevei* (Grunow) Bukhtiyarova**	2.4456	-0.2184	1.5185	2.907
Psammothidium* cf. *chlidanos	0.9973	1.9738	2.4538	2.2212
***Sellaphora nyassensis* (O.Müller) D.G.Mann**	1.0448	-0.1426	2.8523	3.1133

Amphora copulata **(Kützing) Schoeman et Archibald**	1.0518	0.764	2.1086	0.7771
Hantzschia amphioxys **(Ehrenberg) Grunow**	3.9959	0.6952	1.2541	1.3127
Epithemia adnata **(Kützing) Brébisson**	2.4867	-1.2679	1.7395	3.4653
Achnanthes subhudsonis **Hustedt**	1.5792	-0.0797	2.7782	2.7915
Gomphocymbella becarii **(Grunow) Forti**	2.2066	2.3656	3.0954	4.7333
Rhopalodia **sp. Malawi**	2.6534	2.4522	3.2281	3.0456
Surriella nyassae **O. Müller**	1.2205	1.0795	2.152	3.0297

Supporting Documents Table 4. Palynological analyses of core 1C showing pollen percentage data not included in Figure 3. Data included samples at millennial-scale resolution between 120-75 ka with lower-resolution sampling throughout the last 70 ka. Cyp=Cyperaceae; Com=Compositae; Ama=Amaranthaceae; Mim=Mimosaceae; Mac=*Macaranga*; Alc=*Alchornea*; Myr=*Myrica*; Cel=*Celtis*; Fau=*Faurea*; Ixo=*Ixora*; Ant=*Anthocleista*; Aca=*Acalypha*; Cob=Combretaceae; Iso=*Isoberlinia*; Oth=Other Taxa; Typ=*Typha*; Pte=Pteridophytes; Unk=Unknown; Bro=Broken/Crumpled. Taxa in "Other Taxa" include: *Acanthaceae*-type, *Adansonia Aeschynome*-type, *Blighia, Bridelia Canthium, Cassia*-type,*Commiphora*, *Craterispermum*, *Cordia*-type, *Dioscorea, Diospyros*, *Drypetes, Elaeis*-type, *Hyphaene*-type, *Landolfia, Lannea, Mimusops, Neoboutonia*-type, *Phyllanthus*, *Phoenix, Rhus* spp., *Strombosia,* and *Trema,*. Mimosaceae were tallied as monads. Pollen percentages for all arboreal and herbaceous taxa (including those in Figure 3) were calculated based on total number of grains counted per sample less pteridophytes and broken/crumpled.

Depth (m)	Age (yr)	Cyp	Com	Ama	Mim	Mac	Alc	Myr	Cel	Fau	Ixo	Ant	Aca	Cob	Iso	Oth	Typ	Pte	Unk	Bro
3.97	4934	20.7	1.4	0.5	0.0	0.2	0.2	1.4	0.2	0.0	0.0	0.2	2.2	0.5	0.0	3.9	0.0	4.1	5.1	8.2
8.01	13965	16.2	1.4	0.8	0.0	1.8	0.8	0.6	2.1	0.5	1.2	0.5	2.0	0.9	0.0	9.6	2.3	3.5	3.8	5.5
9.14	16984	15.8	2.5	0.6	0.0	1.9	0.9	0.5	0.0	0.2	0.5	0.3	4.3	1.5	0.0	5.1	1.0	4.9	3.2	7.8
10.62	19663	16.8	3.5	0.7	0.0	2.0	0.6	0.9	0.1	0.0	0.3	0.3	3.5	1.1	0.0	5.3	0.0	5.6	3.9	8.2
11.06	22424	15.0	1.4	0.0	0.0	1.2	0.7	1.6	0.2	0.0	0.0	0.4	2.3	1.4	0.0	4.7	0.0	3.0	6.7	11.0
13.05	28306	13.4	2.4	1.2	0.1	0.5	0.5	1.2	0.3	0.3	0.2	0.2	2.1	1.0	0.0	11.0	0.0	9.8	6.8	10.1
18.11	42959	17.3	0.2	0.3	0.3	0.5	1.3	0.5	0.0	0.0	0.2	0.3	1.7	0.8	0.0	6.8	0.0	6.4	5.2	6.3
22.07	52490	9.8	1.2	0.0	0.0	1.8	0.9	0.2	1.5	0.5	3.7	0.2	2.4	0.9	0.0	6.9	1.8	4.0	2.4	4.0
31.07	64987	5.9	0.3	0.2	0.0	1.1	1.0	0.2	2.1	0.2	0.2	0.2	5.2	2.2	0.0	7.4	1.3	1.8	2.9	4.0
32.03	66291	6.3	0.7	2.3	0.2	0.8	1.3	0.0	0.5	0.0	0.0	0.5	1.8	3.0	0.0	0.0	0.8	2.2	5.5	7.5
34.05	69033	4.5	0.0	0.6	0.0	1.1	1.7	0.0	3.0	0.0	0.3	0.3	3.0	1.3	0.0	7.0	1.1	2.7	3.3	4.5
37.02	73053	0.6	9.4	0.2	4.2	0.5	2.7	0.3	3.4	0.3	1.9	0.8	2.5	0.8	0.0	0.0	1.1	9.4	2.8	5.8
39.10	75914	0.5	3.4	0.7	8.5	0.7	3.2	0.0	7.1	0.0	0.0	1.7	3.2	4.4	0.2	1.0	1.7	0.2	4.4	5.4
40.08	77239	0.5	1.7	0.0	1.7	1.7	0.8	0.0	2.6	0.3	0.3	3.6	3.5	2.8	0.0	0.2	0.0	0.0	3.1	4.1
41.04	78539	2.7	0.2	0.4	1.8	0.0	7.8	0.0	3.4	0.0	0.0	0.9	0.9	2.2	0.0	1.6	0.0	0.2	4.5	7.8
43.51	81898	1.0	0.3	0.2	0.0	1.0	1.2	0.3	0.7	0.2	0.0	3.8	2.7	7.6	0.0	3.5	0.0	0.5	1.7	3.3
43.97	82524	0.3	0.2	0.2	0.2	0.3	0.7	0.0	1.6	0.0	0.0	1.5	1.8	1.5	0.0	1.1	1.0	0.3	1.5	4.4
44.95	83860	0.3	0.3	0.5	0.3	0.8	0.3	0.0	1.8	0.2	0.3	0.8	2.0	1.1	0.0	3.9	1.0	1.1	1.8	3.6
46.07	85391	1.3	0.3	0.5	0.2	0.2	0.2	0.0	3.1	0.0	0.0	0.7	1.8	1.0	0.0	3.9	1.8	0.0	2.5	13.6
47.03	86696	0.2	0.0	0.5	0.0	0.5	0.3	0.2	1.0	0.2	0.0	0.7	0.8	0.5	0.0	2.0	0.0	0.0	1.0	4.3
47.97	87972	0.0	0.7	0.8	0.3	0.5	0.3	0.0	2.1	0.0	0.0	0.5	1.3	1.1	0.0	1.0	0.5	0.7	1.1	4.7
49.01	89381	1.0	0.3	0.8	0.3	0.0	0.2	0.3	1.8	0.0	0.0	0.5	0.6	1.1	0.0	1.1	0.5	0.8	1.0	6.6
50.07	90823	0.4	0.7	1.1	0.0	0.0	0.0	0.0	1.1	0.4	0.0	0.0	0.7	0.0	0.4	0.0	0.4	1.9	2.6	8.6
53.48	95464	0.0	0.0	1.1	0.0	0.0	0.0	2.2	2.2	0.0	1.1	0.0	1.1	0.0	0.0	5.4	2.2	0.0	1.1	17.4
54.11	96320	0.0	1.5	0.0	0.0	0.0	0.7	0.7	0.0	0.7	0.7	0.0	2.2	0.7	0.0	0.7	0.0	2.9	0.7	12.5
55.07	97624	0.0	1.2	1.8	0.0	0.0	0.0	0.6	0.6	0.0	0.0	0.0	1.8	0.0	0.0	0.0	0.0	1.2	0.6	10.7
56.03	98935	3.5	2.6	2.2	2.2	0.4	0.4	0.9	1.8	0.0	0.4	0.0	0.4	0.0	0.0	1.8	1.3	8.8	4.8	14.0
57.06	100328	0.2	0.0	0.0	0.0	0.2	0.0	0.0	1.5	0.0	0.0	0.0	1.7	0.0	0.0	0.2	0.0	6.2	1.7	8.7
57.95	101548	0.2	0.0	0.2	0.6	0.0	0.0	0.0	6.2	0.4	0.0	0.4	1.2	0.0	0.0	1.6	3.1	2.3	2.3	3.9
59.00	102976	2.0	0.6	0.0	1.0	0.3	0.0	0.0	2.7	0.0	0.0	1.0	0.7	0.0	0.0	4.4	1.7	4.0	4.4	12.1
60.03	104376	0.7	0.2	0.0	0.0	0.0	0.2	0.3	1.8	0.0	0.0	0.2	1.8	0.2	0.0	0.3	0.0	4.0	1.3	6.3
61.01	105702	2.5	0.2	0.0	1.6	0.3	0.0	0.0	1.6	0.2	0.5	1.0	0.0	0.0	0.0	6.8	1.7	5.5	3.0	3.8
61.98	107018	1.6	0.3	0.2	0.2	0.6	0.0	0.0	2.6	0.8	0.2	0.3	0.9	0.3	0.0	0.9	0.5	8.1	1.6	7.9
63.52	109124	3.9	0.3	0.0	0.0	0.7	0.8	0.0	0.8	0.8	0.7	0.7	0.8	0.8	0.0	2.1	0.7	8.0	2.0	5.9
64.36	110256	5.8	0.5	0.1	0.5	0.5	0.0	0.0	4.9	0.4	1.1	0.1	1.5	0.1	0.0	3.9	4.2	4.7	2.7	8.5
65.25	111467	5.1	0.6	0.0	0.0	1.0	1.1	0.5	1.4	0.2	0.3	1.3	2.9	1.0	0.0	2.7	1.3	5.5	2.4	5.6

66.20	112764	0.5	16.9	0.2	0.0	0.5	0.8	0.0	0.5	0.5	0.0	0.2	0.5	0.6	0.0	1.8	1.4	3.1	3.7	7.7
66.97	113816	5.8	0.3	0.3	0.5	1.0	0.5	0.5	0.3	0.3	1.0	0.0	1.0	0.3	0.2	5.0	2.8	1.5	3.6	4.0
67.37	114361	11.9	0.6	0.0	0.0	0.7	1.0	0.7	0.0	1.0	1.5	0.9	1.2	0.1	0.0	1.0	1.5	4.2	2.2	5.5
71.06	119368	2.9	0.6	2.3	0.3	0.0	0.3	0.0	0.9	0.3	0.0	0.0	1.2	0.9	0.0	0.0	0.0	0.3	7.0	14.8

References

1. Scholz, CA, Johnson, TC, Cohen, AS, King, JW, Peck, J, Overpeck, JT, Talbot, MR, Brown, ET, Kalindekafe, L, Amoako, P, et al. (2007, in press) *Proc. Nat. Acad. Sci.*
2. Sapota, T, Aldahan, A & Al-Aasm, IS (2006) *J. Paleolim.* 36:245-257.
3. Kalindekafe, LS (1993) *J. Afr. Earth Sci.* 17:183-192.
4. Mothersill, JS (1996) in *The Limnology, Climatology and Paleoclimatology of the East African Lakes*, ed. Johnson, TC & Odada, E (Gordon and Breach, Amsterdam), pp. 543-548.
5. Bennett, KD (1996) *New Phytologist* 132:155-170.
6. Spigel, RH & Coulter, GW (1996) in *The Limnology, Climatology and Paleoclimatology of the East African Lakes*, ed. Johnson, TC & Odada, E (Gordon and Breach, Amsterdam), pp. 103-139.
7. Soreghan, MR & Cohen, AS (1996) *Amer. Assoc. Petrol. Geol. Bull.* 80:382-409.
8. Kocher, TD (2004). *Nature Rev. Gen.* 5:288-298.
9. Lehman, JT, Mugidde, R, & Lehman, DA (1998) in *Environmental Change and Response in East African Lakes*, ed. Lehman, JT (Kluwer, Dordrecht), pp. 99-116.
10. Seehausen, O, van Alphen, JJ, & Witte, F (1997) *Science* 277:1808-1811.
11. Johnson, TC, Scholz, CA, Talbot, MR, Kelts, K, Ricketts, RD, Ngobi, G, Beuning, K, Ssemmanda, I & McGill, JW (1996) *Science*, 273:1091-1093.
12. Powers, LA, Johnson, TC, Werne, JP and Castañeda, IS (2005) *Geophys. Res. Let.* 32 doi:10.1029/2004GL022014.
13. Felton, AA, Russell, JM, Cohen, AS, Baker, ME, Chesley, JT, Lezzar, KE, McGlue, MM, Pigati, JS, Quade, J., Stager, JC & Tiercelin, JJ (2007) *Palaeogeog. Palaeoclim. Palaeoecol.* doi:10.1016/j.palaeo.2007.04.003